

## Research Paper

# Interaction of Native Bile Acids with Human Apical Sodium-Dependent Bile Acid Transporter (hASBT): Influence of Steroidal Hydroxylation Pattern and C-24 Conjugation

Anand Balakrishnan,<sup>1</sup> Stephen A. Wring,<sup>2</sup> and James E. Polli<sup>1,3</sup>

Received December 1, 2005; accepted February 10, 2006

**Purpose.** The human apical sodium-dependent bile acid transporter (hASBT) is a potential target for drug delivery, but an understanding of hASBT substrate requirements is lacking. The objective of this study was to characterize hASBT interaction with its native substrates, bile acids, and to evaluate C-24 conjugation and steroidal hydroxylation on transport affinity and inhibition potency.

**Methods.** Transport and inhibition kinetics of 15 bile acids were evaluated (cholate, chenodeoxycholate, deoxycholate, ursodeoxycholate, and lithocholate, including their glycine and taurine conjugates) with an hASBT–Madin-Darby canine kidney (MDCK) monolayer assay. Samples were analyzed via liquid chromatography–mass spectrometry (LC-MS) or chromatography–mass spectrometry–mass spectrometry (LC-MS-MS).

**Results.** C-24 conjugation improved the inhibitory potency of all native bile acids. There was an inverse association between number of steroidal hydroxyl groups and inhibitory potency. Glycolithocholate and tauroolithocholate were the most potent inhibitors. Results from transport studies followed trends from inhibition studies. Conjugated dihydroxy and monohydroxy bile acids exhibited the highest hASBT-mediated transport (i.e., lower  $K_t$  and higher  $J_{max}$ ). Across the 15 bile acids,  $K_t$  generally followed  $K_i$ . Additionally,  $J_{max}$  correlated with  $K_i$ , where greater inhibition potency was associated with higher transport capacity.

**Conclusion.** C-24 conjugation and steroidal hydroxylation pattern modulated native bile acid interaction with hASBT, with C-24 effect dominating steroidal hydroxylation effect. Results indicate that bile acid binding to hASBT may be the rate-limiting step in the apical transport of bile acids.

**KEY WORDS:** ASBT; bile acid; prodrug; QSAR; SLC10A2; transporter.

## INTRODUCTION

The human ileal bile acid transporter, also known as human apical sodium-dependent bile acid transporter (hASBT, SLC10A2), is a key component in the enterohepatic recirculation of bile acids as well as a target for enhanced oral drug absorption (1,2). Structural information on hASBT has been restricted to its primary sequence and membrane

topology (3). In the absence of a high-resolution crystal structure for hASBT, little is known about the interaction of hASBT with its substrates. As a result, the substrate requirements for hASBT are not well developed.

Lack (4) first described a structure–transport relationship for intestinal bile acid transport using the rat everted sac model. These and subsequent observations were based on isolated tissue and organ preparations from animals, where bile acid transport was confounded with other intestinal and hepatic transporters. Evaluation of the literature shows lack of agreement across studies from different research groups regarding hASBT substrate requirements, which seems to reflect the lack of a preferred assay system (5–7). Additionally, native bile acids lack a chromophore, yielding analytical challenges (e.g., lack of sensitivity).

The general lack of information about hASBT substrate requirements has impeded efforts toward prodrug design targeting hASBT (8). Toward this end, a stably transfected hASBT–MDCK monolayer assay was recently developed to evaluate hASBT-mediated transport of solutes (9). Additionally, methods have been developed to avoid bias in kinetic estimates (e.g.,  $K_i$ ,  $K_t$ ) due to system hydrodynamics (10). These methods are applied here to characterize

<sup>1</sup>Department of Pharmaceutical Sciences, School of Pharmacy, University of Maryland, HSF2, Room 623, 20 Penn Street, Baltimore, Maryland 21201, USA.

<sup>2</sup>Trimeris Inc., Morrisville, North Carolina 27560, USA.

<sup>3</sup>To whom correspondence should be addressed. (e-mail: jpolli@rx.umaryland.edu)

**ABBREVIATIONS:** ABL, aqueous boundary layer; CA, cholate; CDCA, chenodeoxycholate; DCA, deoxycholate; GCA, glycocholate; GCDCA, glycochenodeoxycholate; GDCA, glycodeoxycholate; GUDCA, glyoursodeoxycholate; hASBT, human apical sodium-dependent bile acid transporter; HBSS, Hank's balanced salt solution; MDCK, Madin-Darby canine kidney; SLC, solute carrier family; TCA, taurocholate; TCDCA, taurochenodeoxycholate; TDCA, taurodeoxycholate; TUDCA, taurooursodeoxycholate; UDCA, ursodeoxycholate.

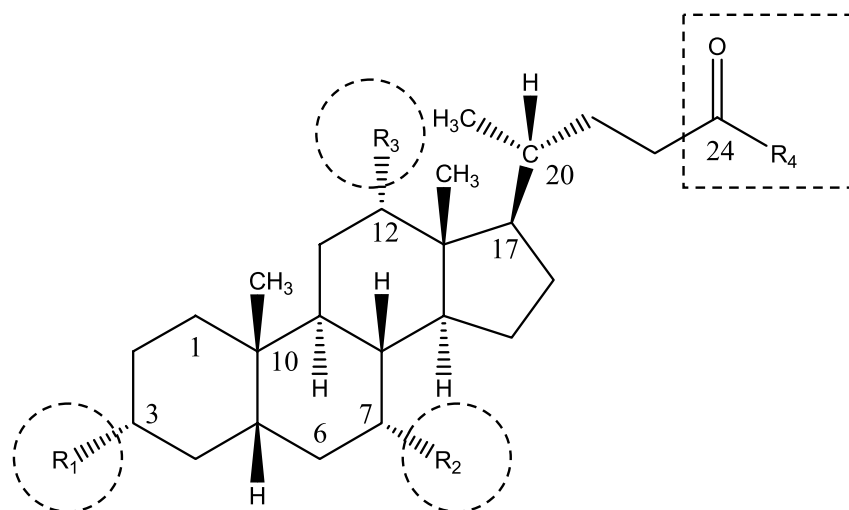


**Fig. 1.** Structure of native bile acids. Bile acids differ in hydroxylation pattern (R1, R2, and R3, as indicated by circles) and in amino acid conjugation pattern at C-24 position (R4, as indicated by the square). Substituent at R-4 is either a free carboxylic acid or conjugate of glycine or taurine.

hASBT interaction with its native substrates, bile acids, including an evaluation of C-24 conjugation and steroidal hydroxylation pattern on transport affinity and inhibition potency.

Native bile acids are the physiological substrates for hASBT and therefore represent an important set of compounds to probe hASBT substrate requirements. Native bile acids vary in steroidal hydroxylation pattern and C-24 conjugation pattern. Figure 1 illustrates the general structure of native bile acids and highlights R1, R2, R3, and R4. Table I describes 15 native bile acids and their differences in hydroxylation (R1, R2, and R3) and C-24 conjugation (R4).

The overall goal of this study was to systematically evaluate the interaction of native bile acids with hASBT and identify chemical features of bile acids that promote interaction with hASBT. Three major objectives are pursued in this study. The first objective was to evaluate the effect of steroidal hydroxylation pattern and C-24 conjugation on the inhibition potency of native bile acids (i.e.,  $K_i$ ). The second objective was to investigate the effect of steroidal hydroxylation and C-24 conjugation on hASBT-mediated transport kinetics (i.e.,  $K_t$  and  $J_{max}$ ). Bile acid structure requirements for hASBT inhibition may differ from requirements for hASBT-mediated transport. Consequently, the third objective was to compare hASBT-inhibition potency vs. kinetic parameters of hASBT-mediated transport.

## METHODS

### Materials

Geneticin, fetal bovine serum, trypsin, and Dulbecco's modified Eagle's medium (DMEM) were purchased from Invitrogen Corporation (Carlsbad, CA, USA). [ $^3\text{H}$ ]Taurocholic acid, [ $^3\text{H}$ ]cholic acid, [ $^{14}\text{C}$ ]chenodeoxycholic acid, [ $^{14}\text{C}$ ]lithocholic acid, and [ $^{14}\text{C}$ ]mannitol were purchased from American Radiolabeled Chemicals (St. Louis, MO,

USA). Glycolithocholic acid, glycooursodeoxycholic acid, and taurooursodeoxycholic acid were obtained from Calbiochem (San Diego, CA, USA). All other chemicals were obtained from Sigma Chemical (St. Louis, MO, USA) or TCI America (Portland, OR, USA).

### Cell Culture

Stably transfected hASBT-MDCK cells were cultured as described previously (9). Briefly, cells were grown at 37°C, 90% relative humidity, and 5% CO<sub>2</sub> atmosphere and fed every 2 days. The medium was DMEM supplemented with 10% fetal bovine serum, 50 U/mL penicillin, and 50 µg/mL

**Table I.** Bile Acid Nomenclature

Bile acid	R <sub>1</sub> (C-3)	R <sub>2</sub> (C-7)	R <sub>3</sub> (C-12)	R <sub>4</sub> (C-24)
CA	-OH	-OH	-OH	-OH
CDCA	-OH	-OH	-H	-OH
DCA	-OH	-H	-OH	-OH
LCA	-OH	-H	-H	-OH
UDCA	-OH	-OH (β)	-H	-OH
GCA	-OH	-OH	-OH	-NHCH <sub>2</sub> COOH
TCA	-OH	-OH	-OH	-NH(CH <sub>2</sub> ) <sub>2</sub> SO <sub>3</sub> H
GCDCA	-OH	-OH	-H	-NHCH <sub>2</sub> COOH
TCDC	-OH	-OH	-H	-NH(CH <sub>2</sub> ) <sub>2</sub> SO <sub>3</sub> H
GDCA	-OH	-H	-OH	-NHCH <sub>2</sub> COOH
TDCA	-OH	-H	-OH	-NH(CH <sub>2</sub> ) <sub>2</sub> SO <sub>3</sub> H
GLCA	-OH	-H	-H	-NHCH <sub>2</sub> COOH
TLCA	-OH	-H	-H	-NH(CH <sub>2</sub> ) <sub>2</sub> SO <sub>3</sub> H
GUDCA	-OH	-OH (β)	-H	-NHCH <sub>2</sub> COOH
TUDCA	-OH	-OH (β)	-H	-NH(CH <sub>2</sub> ) <sub>2</sub> SO <sub>3</sub> H

All hydroxyl (-OH) groups are in the α position, except when noted to be in the β-position. Figure 1 illustrates the structure of bile acids. CA, cholate; CDCA, chenodeoxycholate; DCA, deoxycholate; LCA, lithocholate; UDCA, ursodeoxycholate; GCA, glycocholate; TCA, taurocholate; GCDCA, glycochenodeoxycholate; TCDC, taurochenodeoxycholate; GDCA, glycodeoxycholate; TDCA, taurodeoxycholate; GLCA, glycolithocholate; TLCA, tauroolithocholate; GUDCA, glycooursodeoxycholate; TUDCA, taurooursodeoxycholate.

streptomycin. Geneticin was used at 1 mg/mL to maintain selection pressure. Cells were passaged every 4 days or after reaching 90% confluence.

### Transport across hASBT Monolayers

Transport studies were performed to yield kinetic data that relate to the binding and subsequent translocation across the membrane. hASBT-MDCK cells were grown on polyester Transwells (0.4- $\mu\text{m}$  pore size, 1  $\text{cm}^2$ , Corning, Corning, NY, USA), as described earlier (9). Briefly, cells were seeded at a density of 0.75 million cells/ $\text{cm}^2$  on polyester Transwells and grown under conditions described above. Cells were washed thrice with Hank's balanced salt solution (HBSS) or modified HBSS prior to transport study, and studies were carried out at 37°C at 100 rpm with an orbital shaker. Transport buffer consisted of either HBSS, which contains 137 mM NaCl, or a sodium-free, modified HBSS where sodium chloride was replaced with 137 mM tetraethylammonium chloride. Because bile acid transport is sodium dependent, studies using sodium-free buffer allowed for the measurement of passive transport of bile acids.

Kinetics of hASBT-mediated transport was assessed from transport studies conducted at different donor concentrations of each native bile acid. In all studies, [ $^{14}\text{C}$ ]mannitol was used to monitor monolayer integrity in parallel wells. Mannitol permeability was always less than  $2.5 \times 10^{-6}$  cm/s in each individual well. The apical and basolateral volumes were 0.5 and 1.5 mL, respectively. Samples were quantified using LC-MS or LC-MS-MS, and liquid scintillation counter as described later.

To confirm the absence of organic anion transporting polypeptide (OATP)-mediated transport across hASBT-MDCK cells, taurocholate (TCA) transport was measured in the absence and presence of the OATP substrate bromosulfalein (BSP). No differences were observed in TCA transport in the presence and absence of 100  $\mu\text{M}$  BSP (data not shown).

### Inhibition Studies

hASBT-MDCK cells were seeded at a density of 1.5 million cells/well in 12-well plates (Corning) and induced with 10 mM sodium butyrate for 12–15 h at 37°C prior to study on day 4. Kinetics of hASBT-mediated TCA uptake was assessed from uptake studies ( $n = 3$ ) at differing donor concentrations (1–200  $\mu\text{M}$  spiked with [ $^3\text{H}$ ]TCA) (9). Studies were performed by using HBSS with 10 mM HEPES (pH 6.8) at 37°C and 50 rpm for 10 min. The donor solution was removed and the cells were washed three times with chilled sodium-free buffer. Cells were lysed with 0.25 mL of 1 N NaOH and neutralized with 0.25 mL of 1 N HCl. Cell lysate was then counted for associated radioactivity by using a liquid scintillation counter (Beckman Instruments; Fullerton, CA, USA).

To characterize hASBT binding requirements, cis-inhibition studies of TCA uptake were carried out by using individual native bile acids at various concentrations (0–100  $\mu\text{M}$ ). Cells were exposed to donor solution containing TCA and inhibitor for 10 min. The donor solution was removed and the cells were washed three times with chilled

sodium-free buffer. Cells were lysed and the lysate was counted for associated radioactivity, as described above. Inhibition data were analyzed in terms of inhibition constant  $K_i$ , as described below.

### Analytical Methods

Bile acids were analyzed by means of LC-MS-MS on an Agilent HPLC system, equipped with an autosampler (CTC Analytics, Zwingen, Switzerland) and a Sciex API4000-Qtrap mass spectrometer (Applied Biosystems, Foster City, CA, USA). The column was a Phenomenex Luna C18 (50  $\times$  2 mm, 3  $\mu\text{m}$ ; Phenomenex, Torrance, CA, USA) heated to 40°C. The flow rate was 0.7 mL/min, and the mobile phase contained a gradient of 1–80% acetonitrile in ammonium acetate (pH 6.8). Detection was achieved under negative or positive ion electrospray tandem mass spectrometry using  $[\text{M}-\text{H}]^-$  peak for all the native bile acids, as the  $[\text{M}-\text{H}]^-$  peak provided the greatest sensitivity. Radiolabeled bile acids and mannitol were quantified by using a Beckman liquid scintillation counter model LS 5801 (Beckman Instruments; Fullerton, CA), in Econosafe scintillation cocktail.

### Kinetic Analysis

Flux data were analyzed as described earlier (10). Briefly, flux data were fitted to a previously developed modified Michaelis-Menten model that takes into account aqueous boundary layer (ABL) resistance [Eq. (1)]. Data from sodium-free studies were fitted to a passive transport model [Eq. (2)].

$$J = \frac{P_{\text{ABL}} \cdot \left( \frac{J_{\text{max}}}{K_t + S} + P_p \right) \cdot S}{P_{\text{ABL}} + \frac{J_{\text{max}}}{K_t + S} + P_p} \quad (1)$$

$$J = \frac{P_{\text{ABL}} \cdot P_p \cdot S}{P_{\text{ABL}} + P_p} \quad (2)$$

where  $J$  is TCA flux,  $J_{\text{max}}$  and  $K_t$  are the Michaelis-Menten constants for hASBT-mediated transport,  $S$  is TCA (i.e., substrate) concentration,  $P_p$  is the passive TCA permeability coefficient, and  $P_{\text{ABL}}$  is the ABL permeability. In Eqs. (1) and (2),  $P_{\text{ABL}}$  was  $70 \times 10^{-6}$  cm/s (10). Equations (1) and (2) were applied simultaneously to with sodium and sodium-free flux data to estimate  $K_t$ ,  $J_{\text{max}}$ , and  $P_p$ . A pooled data analysis approach was used to model flux data from multiple studies. The pooled approach entailed fitting Eqs. (1) and (2) to flux data pooled from multiple experiments, to yield a single  $K_t$  estimate across multiple studies;  $J_{\text{max}}$  and  $P_p$  were unique for each study.

Taurocholate flux was measured in each study to serve as a normalizing approach to account for variation in hASBT expression levels between studies. Taurocholate  $J_{\text{max}}$  ranged between 0.000065 to 0.001  $\text{nmol s}^{-1} \text{cm}^{-2}$  across studies. hASBT expression levels can be expected to directly affect  $J_{\text{max}}$  estimates. To correct for variation in hASBT expression levels across studies,  $J_{\text{max}}$  of each bile acid was normalized against TCA  $J_{\text{max}}$  from the same study, yielding a normalized

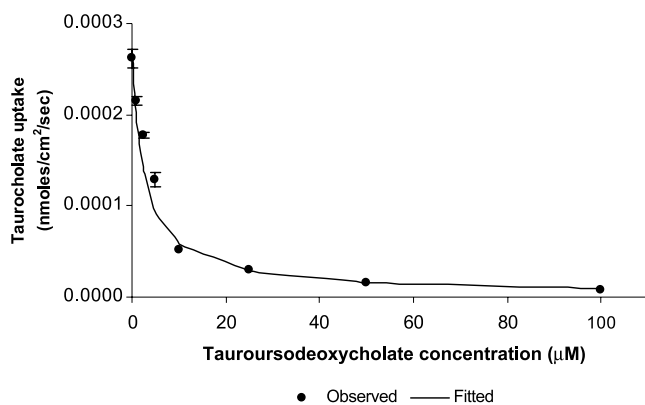


**Fig. 2.** Concentration-dependent inhibition of taurocholate (TCA) uptake into hASBT-MDCK monolayers by tauroursodeoxycholate. Cis-inhibition studies of TCA uptake (0.5 M) were carried out at varying concentrations of individual native bile acids. Closed circles indicate observed data points. Solid line indicates model fit. TCA uptake into hASBT-MDCK cells was reduced significantly by tauroursodeoxycholate. Qualitatively similar profiles were observed for each native bile acid. Each point is the mean  $\pm$  SEM of at least three measurements.

$J_{\max}$  for the bile acid of interest. Normalized  $J_{\max}$  that exceed a value of 1 indicate  $J_{\max}$  exceeded the  $J_{\max}$  of TCA. Normalized  $J_{\max}$  less than 1 indicate that  $J_{\max}$  was lower than TCA  $J_{\max}$ .

The following competitive inhibition model was applied to cis inhibition studies of TCA uptake by individual bile acids:

$$J_{\text{ABL}} = \frac{P_{\text{ABL}} \cdot \left( \frac{J_{\max}}{K_i(1+I/K_i)+S} + P_p \right) \cdot S}{P_{\text{ABL}} + \left( \frac{J_{\max}}{K_i(1+I/K_i)+S} \right) + P_p} \quad (3)$$

where  $I$  is the concentration of inhibitor (i.e., inhibitory bile acid) and  $S$  is the concentration of TCA (i.e., 0.5 or 5  $\mu\text{M}$ ). In applying Eq. (3), only  $K_i$  was estimated. The other three parameters (i.e.,  $J_{\max}$ ,  $K_t$ , and  $P_p$ ) were estimated from TCA uptake studies without inhibitor using Eqs. (1) and (2).

### Statistical Analysis

Nonlinear curve fitting was performed by using Win-Nonlin 4.1 (Pharsight, Mountain View, CA, USA). Results were analyzed by Student's  $t$  test and ANOVA. A  $p$  value of less than 0.05 was considered significant. SEM of a ratio was calculated by using the delta method (11).

## RESULTS

### Inhibition Studies

Each bile acid inhibited TCA uptake into hASBT-MDCK in a concentration-dependent fashion. For example, Fig. 2 illustrates the inhibition profile of tauroursodeoxycholate (TUDCA). Similar profiles were observed for all other native bile acids. Glycine and taurine conjugates of lithocholate exhibited the greatest inhibitory potency with  $K_i$  estimates of about 0.5  $\mu\text{M}$ . Ursodeoxycholate (UDCA) and cholate (CA) were the least potent compounds with  $K_i$  estimates of approximately 20  $\mu\text{M}$ .

Table II lists the  $K_i$  values for the unconjugated, glycine conjugate, and taurine conjugate of five parent bile acids. These five parent bile acids differ in steroidal hydroxylation pattern, although each possesses a C-3  $\alpha$ -OH. Cholate is a trihydroxy bile acid. UDCA, deoxycholate (DCA), and chenodeoxycholate (CDCA) are dihydroxy bile acids. Lithocholate is a monohydroxy bile acid.

For each parent bile acid, glycine or taurine conjugation at C-24 enhanced inhibition potency (i.e., lowered  $K_i$ ). For CA, glycine and taurine conjugation resulted in a 2- and 3-fold enhancement in inhibitory potency, respectively. Similarly, for the dihydroxy bile acids CDCA and DCA, glycine and taurine conjugates enhanced potency 2-fold. UDCA exhibited the greatest sensitivity to conjugation, with glycine and taurine conjugates providing 7- and 22-fold enhancement in inhibition potency, respectively. Conjugates of lithocholate exhibited 4-fold greater inhibition potency than unconjugated lithocholate. In general, glycine and taurine enhanced inhibitory potency of parent bile acids to similar extents.

Inhibitory potency generally exhibited an inverse relationship with number of hydroxyl groups, with the dihydroxy and monohydroxy bile acids exhibiting greater potency than trihydroxy bile acids. Across unconjugated bile acids, CDCA and lithocholate exhibited the greatest inhibitory potency with  $K_i$  value of 2  $\mu\text{M}$ . CA and UDCA exhibited the lowest inhibitory potency with  $K_i$  values of 17 and 22  $\mu\text{M}$ , respectively. The dihydroxy bile acids DCA, CDCA, and UDCA differed with respect to the location and orientation of the second hydroxyl group (Table I). Among these three dihydroxy bile acids, CDCA exhibited the greatest potency ( $K_i = 2 \mu\text{M}$ ). Its C-7  $\beta$ -OH epimer, UDCA, yielded a  $K_i$  of 22  $\mu\text{M}$ . DCA exhibited a modestly lower potency ( $K_i = 8 \mu\text{M}$ ) and possesses the second hydroxyl group at C-12. Steroidal hydroxylation pattern also influenced C-24 conjugated bile acids and mirrored the effect observed in unconjugated bile acids. Among conjugates, monohydroxy bile acids exhibited

**Table II.** Effect of C-24 Conjugation Steroidal Hydroxylation Pattern on Inhibition Potency of Native Bile Acids

Hydroxylation pattern	Parent bile acid	$K_i$ ( $\mu\text{M}$ )		
		Unconjugated	Glycine	Taurine
Trihydroxy (3 $\alpha$ , 7 $\alpha$ , 12 $\alpha$ )	Cholate	17.7 ( $\pm 1.4$ )	7.53 ( $\pm 0.44$ )	4.96 ( $\pm 0.17$ )
Dihydroxy (3 $\alpha$ , 12 $\alpha$ )	Deoxycholate	8.31 ( $\pm 0.77$ )	3.22 ( $\pm 0.26$ )	3.19 ( $\pm 0.16$ )
Dihydroxy (3 $\alpha$ , 7 $\alpha$ )	Chenodeoxycholate	1.94 ( $\pm 0.17$ )	0.992 ( $\pm 0.089$ )	0.933 ( $\pm 0.096$ )
Dihydroxy (3 $\alpha$ , 7 $\beta$ )	Ursodeoxycholate	22.6 ( $\pm 3.0$ )	3.41 ( $\pm 0.21$ )	0.819 ( $\pm 0.046$ )
Monohydroxy (3 $\alpha$ )	Lithocholate	2.10 ( $\pm 0.22$ )	0.427 ( $\pm 0.017$ )	0.50 ( $\pm 0.052$ )

Values in parenthesis indicate SEM ( $n = 3$ ).

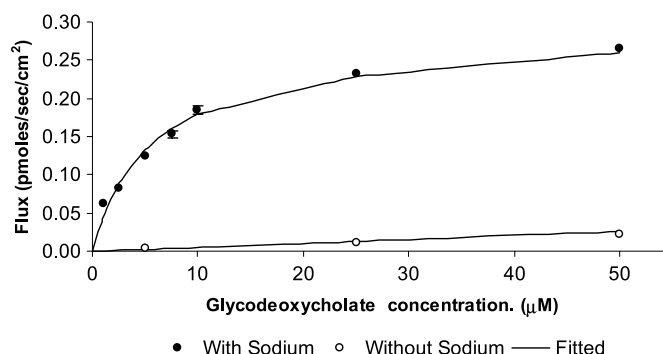


**Fig. 3.** Concentration-dependent transport of glycodeoxycholate (GDCA) across hASBT-MDCK monolayers. GDCA flux was measured at varying donor concentrations (1–50  $\mu\text{M}$ ) in the presence and absence of sodium to delineate hASBT-mediated and passive components of flux. Filled circles represent flux data in the presence of sodium. Open circles represent passive flux (i.e., absence of sodium). The solid lines represent model fits. In the presence of sodium, GDCA transport was significantly larger compared to transport in the absence of sodium. Similar profiles were obtained for other conjugated bile acids and cholic acid. Unconjugated dihydroxy and monohydroxy bile acids exhibited high passive flux, such that active flux was not discerned. Each point is the mean  $\pm$  SEM of at least three measurements.

the greatest potency, followed by dihydroxy and trihydroxy bile acids. Glycine and taurine conjugates of lithocholate exhibited the greatest potency with  $K_i$  estimates of about 0.5  $\mu\text{M}$ . The dihydroxy bile acid conjugates generally exhibited potency that were within about 3-fold of each other (i.e., between 1 and 3  $\mu\text{M}$ ). In general, steroidal hydroxylation effects in conjugated bile acids were less prominent compared to their effects in unconjugated bile acids. This pattern indicates that C-24 conjugation dominated hydroxylation effects in determining inhibitory potency. This pattern is most evident for UDCA ( $K_i = 22 \mu\text{M}$ ), where taurine conjugation enhances potency 22-fold ( $K_i = 0.82 \mu\text{M}$ ).

### Transport Studies

Each of the 15 native bile acids can be expected to exhibit hASBT-mediated transport. For example, Fig. 3 illustrates the concentration-dependent transport of glycodeoxycholate (GDCA) across hASBT-MDCK monolayers. GDCA transport was mediated largely by hASBT, with an approximately 20-fold greater flux from sodium-containing studies than from sodium-free studies. Similar profiles were obtained for all conjugated bile acids and CA, such that 11 of the 15 bile acids exhibited significant hASBT-mediated transport. The unconjugated forms of the three dihydroxy

**Table III.** Kinetic Estimates of hASBT-Mediated Transport of Unconjugated and Glycine/Taurine Conjugates of Bile Acids

Parent bile acid	C-24 conjugate	Normalized $J_{\max}$	$K_t$ ( $\mu\text{M}$ )	$P_p$ (cm/s) $\times 10^6$
Cholate	Unconjugated	0.714 (0.028)	15.1 (1.4)	0.962 (0.005)
	Glycine	1.52 (0.24)	11.0 (1.9)	0.220 (0.157)
	Taurine	1.00 (0.18)	4.39 (0.29)	1.15 (0.11)
Ursodeoxycholate	Unconjugated <sup>a</sup>	nm	nm	21.2 (0.9)
	Glycine	2.26 (0.36)	11.5 (2.0)	1.01 (0.13)
	Taurine	2.21 (0.68)	10.3 (4.0)	1.00 (6.32)
Deoxycholate	Unconjugated <sup>b</sup>	nm	nm	23.8 (0.4)
	Glycine	3.49 (0.47)	1.10 (0.26)	0.520 (0.162)
	Taurine	1.75 (0.11)	0.497 (0.147)	2.47 (0.14)
Chenodeoxycholate	Unconjugated <sup>c</sup>	nm	nm	20.7 (0.7)
	Glycine	4.32 (0.58)	0.662 (0.337)	0.414 (0.201)
	Taurine	3.47 (0.46)	<0.1	0.923 (0.013)
Lithocholate	Unconjugated <sup>d</sup>	nm	nm	14.2 (0.3)
	Glycine	4.05 (0.64)	<0.1	0.865 (0.780)
	Taurine	8.50 (2.11)	8.43 (3.10)	0.020 (0.263)

Values in parenthesis indicate SEM ( $n = 3$ ). nm = not measurable due to high passive permeability.

<sup>a</sup> Permeability of ursodeoxycholate in the presence of sodium was  $23.8 (0.3) \times 10^{-6}$  cm/s.

<sup>b</sup> Permeability of deoxycholate in the presence of sodium was  $30.9 (0.2) \times 10^{-6}$  cm/s.

<sup>c</sup> Permeability of chenodeoxycholate in the presence of sodium was  $23.9 (0.4) \times 10^{-6}$  cm/s.

<sup>d</sup> Permeability of lithocholate in the presence of sodium was  $12.4 (0.3) \times 10^{-6}$  cm/s.

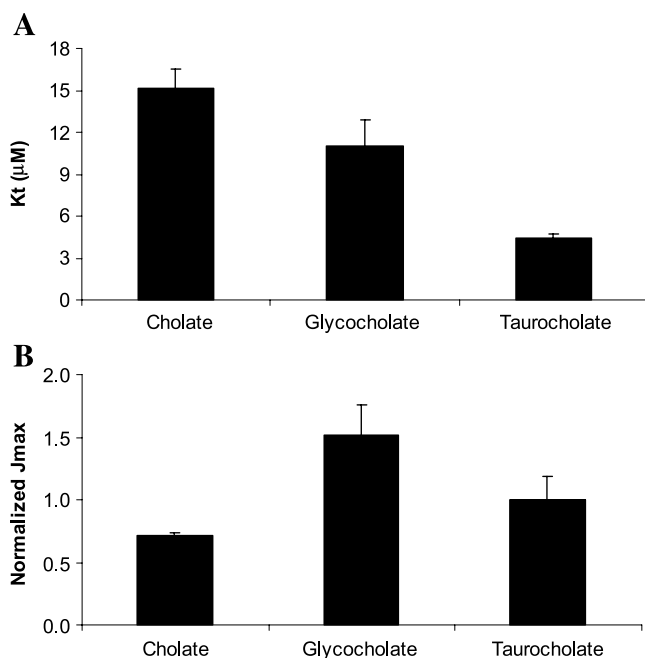


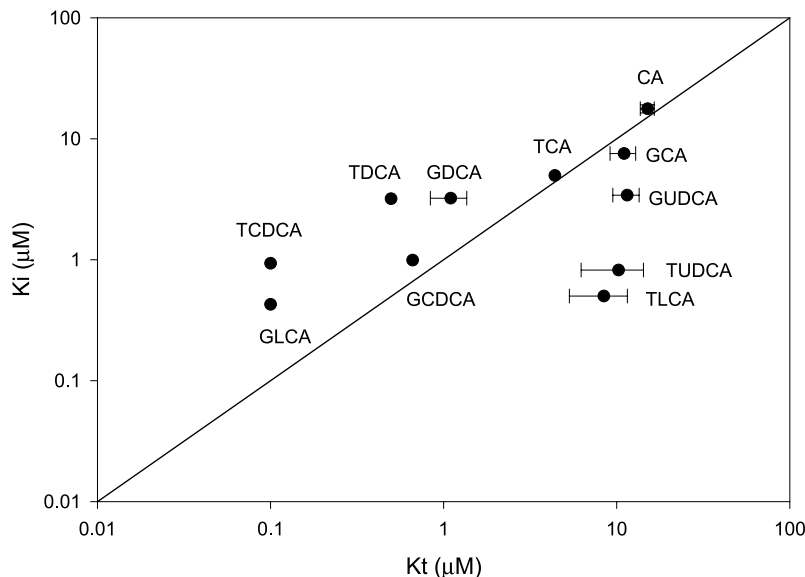
**Fig. 4.** Effect of C-24 conjugation on  $K_t$  and  $J_{\text{max}}$  of cholate and its conjugates. (A) Effect on  $K_t$ , (B) effect on  $J_{\text{max}}$ . In (A), conjugation at C-24 improved the affinity relative to cholic acid, with taurine conjugates exhibiting the greatest affinity. This conjugation effect was similar to inhibition results (Fig. 3). In (B), C-24 conjugation had no patterned effect on  $J_{\text{max}}$ . Each point is the mean  $\pm$  SEM of at least three measurements.

bile acids and the monohydroxy bile acid lithocholate did not show apparent hASBT-mediated transport, perhaps due to their high passive permeability (12).

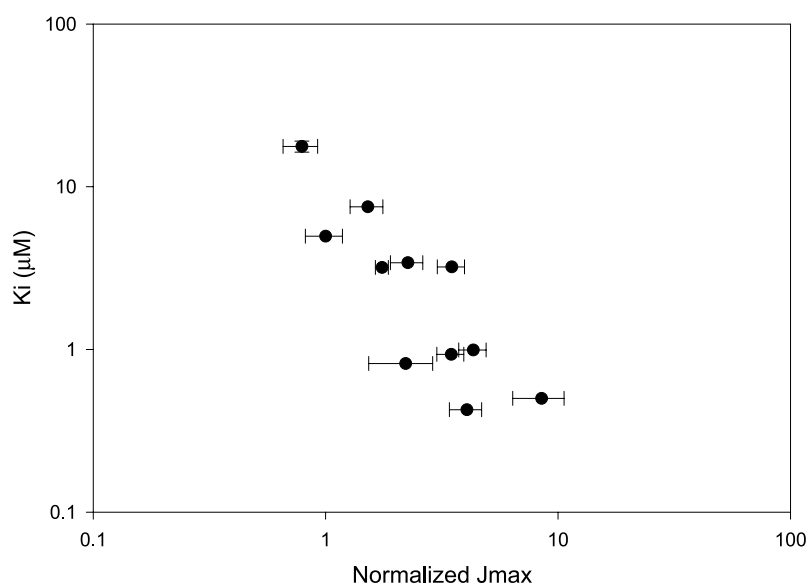
Table III lists the transport parameters of five parent bile acids and their glycine and taurine conjugates. Kinetic parameters include normalized  $J_{\text{max}}$ ,  $K_t$ , and  $P_p$ .  $K_t$  represents the Michaelis-Menten parameter for hASBT. Normalized  $J_{\text{max}}$  is  $J_{\text{max}}$ , relative to TCA  $J_{\text{max}}$ . For example, a normalized  $J_{\text{max}}$  of 2.0 indicates a  $J_{\text{max}}$  that is 2-fold the TCA  $J_{\text{max}}$ .  $P_p$  refers to passive permeability. In Table III, unconjugated dihydroxy and monohydroxy bile acids exhibited high passive permeability, which seems to mask hASBT-mediated flux. Hence,  $K_t$  and  $J_{\text{max}}$  were not measurable for these four bile acids.

Figure 4 illustrates the effect of C-24 conjugation on hASBT-mediated transport of CA, which was the only unconjugated bile acid to exhibit measurable hASBT-mediated transport. In Fig. 4A, glycine and taurine conjugation generally enhanced affinity (i.e., lowered  $K_t$ ). Taurocholate exhibited the greatest affinity with  $K_t = 4.39 \mu\text{M}$ , which is approximately 3.5-fold lower than unconjugated CA ( $K_t = 15.1 \mu\text{M}$ ). This trend is qualitatively similar to inhibition data (Table II). In Fig. 4B, conjugation did not impact  $J_{\text{max}}$  in a consistent fashion relative to unconjugated CA, although  $J_{\text{max}}$  was generally higher for conjugates.

Across the various bile acids, affinities of glycine conjugates were generally the same as the affinities of taurine conjugates, except for CA conjugates. Hence, although C-24 conjugation enhanced affinity, neither conjugate was more effective. Normalized  $J_{\text{max}}$  estimates were essentially the same across both glycine and taurine conjugates.



**Fig. 5.** Comparison of  $K_i$  and  $K_t$  estimates for native bile acids. Qualitatively, most bile acids yielded  $K_i$  and  $K_t$  values that were similar to one another (i.e., within 5-fold similar). Four bile acids yielded  $K_i$  and  $K_t$  estimates that differed by more than 5-fold, although were within 20-fold of each other. Tauroolithocholate (TLCA) and taurourso-deoxycholate (TUDCA) yielded  $K_i$  values that were over 5-fold more potent than  $K_t$ . Meanwhile, taurochenodeoxycholate (TCDCA) and glycolithocholate (GLCA) yielded  $K_i$  values that were over 5-fold more potent than  $K_t$ . Each point is the mean  $\pm$  SEM of at least three measurements. CA, cholate; GCA, glycocholate; GCDCA, glycochenodeoxycholate; GDCA, glycodeoxycholate; GUDCA, glycourso-deoxycholate; TCA, taurocholate; TDCA, taurodeoxycholate.



**Fig. 6.** Relationship between  $K_i$  and  $J_{max}$ . Higher capacity (i.e.,  $J_{max}$ ) was associated with greater inhibitory potency. Each point is the mean  $\pm$  SEM of at least three measurements.

In comparing the effects of steroidal hydroxylation pattern, an inverse relationship was observed between transport affinity ( $K_t$ ) and the number of steroidal hydroxyl groups (Table III). Dihydroxy and monohydroxy bile acids generally exhibited greater affinity than trihydroxy bile acids. Conjugates of dihydroxy bile acids DCA and CDCA exhibited very high affinity, with  $K_t$  estimates less than 1  $\mu$ M. Similarly, glycine conjugate of lithocholate also exhibited high affinity with  $K_t$  less than 1  $\mu$ M. UDCA conjugates exhibited a 10-fold poorer affinity than its epimer CDCA, indicating the C-7  $\beta$ -OH is less favorable than the C-7  $\alpha$ -OH. Normalized  $J_{max}$  exhibited a modest inverse association with the number of steroidal hydroxyl groups. Cholate conjugates showed normalized  $J_{max}$  values of about 1.0, whereas normalized  $J_{max}$  of the dihydroxy and monohydroxy bile acids exhibited normalized  $J_{max}$  about over 4-fold higher. In summary, dihydroxy and monohydroxy conjugates exhibited both greater affinity and higher  $J_{max}$  compared to trihydroxy conjugates.

#### Comparison of Inhibition Kinetics vs. Transport Kinetics

hASBT inhibition requirements can be expected to differ from hASBT-mediated transport requirements. For example, a compound may be a better inhibitor than substrate. Figure 5 compares inhibitory potency ( $K_i$ ) against transport affinity ( $K_t$ ) for each bile acid. Overall, all bile acids were potent inhibitors ( $K_i$  ranging from about 0.5 to 15  $\mu$ M) and potent substrates ( $K_t$  ranging from about 0.1 to about 15  $\mu$ M). Qualitatively, most bile acids yielded  $K_i$  and  $K_t$  values that were similar to one another (i.e., within 5-fold). Two bile acids were more potent as inhibitors than as substrates (i.e.,  $K_i$  lower than  $K_t$ ). These two bile acids were tauroolithocholate (TLCA) and TUDCA and fall below the line of unity in Fig. 5. Each is a taurine conjugate with an  $\alpha$ -OH at only the C-3 position. Meanwhile, taurochenodeoxycholate (TCDCA) and glycolithocholate (GLCA) exhibited  $K_t$  values that were more than 5-fold lower than  $K_i$  estimates

(i.e., points above the line of unity in Fig. 5). Both TCDCA and GLCA exhibited  $K_i$  less than 1.0  $\mu$ M and also exhibited  $K_t$  less than 1.0  $\mu$ M; hence, there was qualitative agreement between  $K_i$  and  $K_t$  values for TCDCA and GLCA.

Figure 6 compares normalized  $J_{max}$  to inhibitory potency. There was an inverse association between  $K_i$  and normalized  $J_{max}$ , indicating that among the studied native bile acids, potent inhibitors generally exhibit a greater  $J_{max}$ .

#### DISCUSSION

The scope of the present study was to characterize hASBT-mediated transport and inhibition characteristics of native bile acids. Current understanding of hASBT substrate requirements is based on studies prior to the cloning of human ASBT and did not lead to a unified model. These studies suffered from various limitations including confounding effects of hepatic transporters and unstirred water layer effects (6). Recent studies have employed cell-based models, including hASBT transfected systems, to delineate hASBT substrate requirements (13–17). Craddock *et al.* (13) developed the hASBT-COS system and characterized several bile acids. Glycodihydroxy bile acids exhibited the greatest transport affinity for hASBT, in apparent contrast to the prevailing hypothesis that trihydroxy bile acids are best transported (4). Using Caco-2 monolayers, Swaan *et al.* (17,18) examined the transport of several C-24 bile acid-peptide conjugates and concluded that the C-24 side chain could be at least 14  $\text{\AA}$  in length and still allow for translocation; large hydrophobic moieties increased binding to hASBT. Cholic acid exhibited a greater affinity (i.e., lower  $K_i$ ) than TCA (15), in contrast to results from Dawson *et al.* (13). The inconsistency of results across studies has led to a poor understanding of the substrate requirements for hASBT, even after the cloning of hASBT. Furthermore, no study has attempted to systematically characterize the interaction of native bile acids with hASBT via both inhibition studies and transport studies.

The current study uses an hASBT–MDCK monolayer model that overexpresses hASBT, thus avoiding confounding effects of other transporters (9). Additionally, ABL effects can be accommodated, yielding  $K_t$  estimates in the micromolar range, in contrast to previous studies where the ABL influences led to biased  $K_t$  estimates (6). Because both inhibition and transport studies were performed, the present study compares the associations between inhibition potency, substrate potency, and transport capacity. No previous study measures these kinetic parameters and investigates these associations for hASBT, or apparently for any transporter.

Interestingly, the most developed pharmacophore for ASBT was developed using a chemical library that did not include bile acids (19). Rather, the library was largely composed of non-bile-acid analogues designed to serve as cholesterol-lowering agents via ASBT inhibition. The assay system employed rabbit ASBT. The resulting 3-D pharmacophore model for ASBT identified five chemical features: one hydrogen bond donor, one hydrogen bond acceptor, and three hydrophobic features. The pharmacophore concerns ASBT inhibition, as data for the model was inhibition data and not transport data. It is also interesting to note that TCA did not map all the features of the pharmacophore (19).

Results in the present study indicate that C-24 conjugation enhanced the inhibitory potency of bile acids (i.e.,  $K_i$ ). This trend was consistent across all bile acids, including trihydroxy, dihydroxy, and monohydroxy bile acids. This report is the first comprehensive attempt to evaluate C-24 conjugation effects across each mono, di-, and trihydroxy bile acids. An inverse relationship was observed between number of hydroxyl groups and inhibitory potency, with monohydroxy bile acids being the most potent inhibitors. Across dihydroxy bile acids, CDCA exhibited greater potency than DCA and UDCA. This pattern indicates that C-7  $\alpha$ -OH is more favorable than C-12  $\alpha$ -OH, which is more favorable than C-7  $\beta$ -OH. C-24 conjugation generally dominated steroidal hydroxylation effects.

Results from transport studies mirrored these trends from inhibition studies. C-24 glycine or taurine conjugation generally enhanced transport affinity in case of cholic acid. Unconjugated dihydroxy and monohydroxy bile acids exhibited high passive permeability and did not exhibit measurable hASBT-mediated transport. Steroidal hydroxylation had a significant effect on transport affinity (i.e.,  $K_t$ ). Fewer hydroxyl groups promoted bile acid interaction with hASBT. The hydroxylation pattern influenced both  $K_t$  and the  $J_{max}$ . Cholate and its conjugates exhibited higher  $K_t$  and lower  $J_{max}$ , whereas CDCA conjugates exhibited lower  $K_t$  and higher  $J_{max}$ . However, overall, all native bile acids showed high affinity for hASBT, as  $K_t$  values were on the order of 1 to 15  $\mu$ M, rather than 1 mM as reported earlier (5).

Translocation of substrate by a transporter is a complex process. Minimally, translocation requires (a) binding of substrate to transporter, (b) vectoral translocation of substrate via change in transporter conformation, (c) dissociation of substrate, and (d) restoration of transporter to binding conformation. This description is a simplistic one, particularly for transporters such as hASBT, which cotransports sodium. Based on the high capacity and high affinity of hASBT-mediated transport of bile acids, we speculate that bile acid binding to hASBT may be the rate-limiting step in the apical

transport of bile acids. In Fig. 6, binding, as assessed by  $K_i$ , seems to determine  $J_{max}$ , suggesting binding is the rate-limiting step in the apical transport of bile acids. This hypothesis would suggest that vectoral translocation of substrate, dissociation of substrate, and restoration of transporter are not rate limiting. A future aim will be the consideration of biophysical data in concert with transport/inhibition kinetic data to better understand hASBT functioning.

## ACKNOWLEDGMENT

This work was supported in part by National Institutes of Health grant DK67530.

## REFERENCES

1. S. Tolle-Sander, K. A. Lentz, D. Y. Maeda, A. Coop, and J. E. Polli. Increased acyclovir oral bioavailability via a bile acid conjugate. *Mol. Pharm.* **1**:40–48 (2004).
2. G. A. Kullak-Ublick, B. Stieger, and P. J. Meier. Enterohepatic bile salt transporters in normal physiology and liver disease. *Gastroenterology* **126**:322–342 (2004).
3. E. Y. Zhang, M. A. Phelps, A. Banerjee, C. M. Khantwal, C. Chang, F. Helsper, and P. W. Swaan. Topology scanning and putative three-dimensional structure of the extracellular binding domains of the apical sodium-dependent bile acid transporter (SLC10A2). *Biochemistry* **43**:11380–11392 (2004).
4. L. Lack. Properties and biological significance of the ileal bile salt transport system. *Environ. Health Perspect.* **33**:79–90 (1979).
5. S. N. Marcus, C. D. Schteingart, M. L. Marquez, A. F. Hofmann, Y. Xia, J. H. Steinbach, H. T. Ton-Nu, J. Lillienau, M. A. Angellotti, and A. Schmassmann. Active absorption of conjugated bile acids *in vivo*. Kinetic parameters and molecular specificity of the ileal transport system in the rat. *Gastroenterology* **100**:212–221 (1991).
6. E. R. Schiff, N. C. Small, and J. M. Dietschy. Characterization of the kinetics of the passive and active transport mechanisms for bile acid absorption in the small intestine and colon of the rat. *J. Clin. Invest.* **51**:1351–1362 (1972).
7. R. Aldini, A. Roda, M. Montagnani, C. Cerre, R. Pellicciari, and E. Roda. Relationship between structure and intestinal absorption of bile acids with a steroid or side-chain modification. *Steroids* **61**:590–597 (1996).
8. B. Hagenbuch and P. Dawson. The sodium bile salt cotransport family SLC10. *Pflugers Arch.* **447**:566–570 (2004).
9. A. Balakrishnan, D. J. Sussman, and J. E. Polli. Development of stably transfected monolayer overexpressing the human apical sodium-dependent bile acid transporter (hASBT). *Pharm. Res.* **22**:1269–1280 (2005).
10. A. Balakrishnan and J. E. Polli. Deleterious effect of high transporter expression in the estimation of transporter kinetics. *AAPS J.* **7**:R6224 (2005).
11. M. A. Tanner. *Tools for Statistical Inference, vol. 67: Lecture Notes in Statistics*, Springer-Verlag, Berlin, 1992.
12. K. A. Lentz, J. W. Polli, S. A. Wring, J. E. Humphreys, and J. E. Polli. Influence of passive permeability on apparent P-glycoprotein kinetics. *Pharm. Res.* **17**:1456–1460 (2000).
13. A. L. Craddock, M. W. Love, R. W. Daniel, L. C. Kirby, H. C. Walters, M. H. Wong, and P. A. Dawson. Expression and transport properties of the human ileal and renal sodium-dependent bile acid transporter. *Am. J. Physiol.* **274**:G157–G169 (1998).
14. C. E. Chandler, L. M. Zaccaro, and J. B. Moberly. Trans-epithelial transport of cholytaurine by Caco-2 cell monolayers is sodium dependent. *Am. J. Physiol.* **264**:G1118–G1125 (1993).
15. M. Kagedahl, P. W. Swaan, C. T. Redemann, M. Tang, C. S. Craik, F. C. Szoka Jr., and S. Oie. Use of the intestinal bile acid transporter for the uptake of cholic acid conjugates with HIV-1 protease inhibitory activity. *Pharm. Res.* **14**:176–180 (1997).



16. W. Kramer, S. Stengelin, K. H. Baringhaus, A. Enhsen, H. Heuer, W. Becker, D. Corsiero, F. Girbig, R. Noll, and C. Weyland. Substrate specificity of the ileal and the hepatic Na(+)/bile acid cotransporters of the rabbit. I. Transport studies with membrane vesicles and cell lines expressing the cloned transporters. *J. Lipid Res.* **40**:1604–1617 (1999).
17. P. W. Swaan, K. M. Hillgren, F. C. Szoka Jr., and S. Oie. Enhanced transepithelial transport of peptides by conjugation to cholic acid. *Bioconjug. Chem.* **8**:520–525 (1997).
18. P. W. Swaan, F. C. Szoka Jr., and S. Oie. Molecular modeling of the intestinal bile acid carrier: a comparative molecular field analysis study. *J. Comput. Aided Mol. Des.* **11**:581–588 (1997).
19. K. H. Baringhaus, H. Matter, S. Stengelin, and W. Kramer. Substrate specificity of the ileal and the hepatic Na(+)/bile acid cotransporters of the rabbit. II. A reliable 3D QSAR pharmacophore model for the ileal Na(+)/bile acid cotransporter. *J. Lipid Res.* **40**:2158–2168 (1999).